

Finite-frequency thermoelectric response in strongly correlated quantum dots

Razvan Chirla^{1,*} and Cătălin Pașcu Moca^{1,2}

¹*Department of Physics, University of Oradea, 410087, Oradea, Romania*

²*BME-MTA Exotic Quantum Phase Group, Institute of Physics,
Budapest University of Technology and Economics, H-1521 Budapest, Hungary*

(Dated: February 12, 2018)

We investigate the finite-frequency thermal transport through a quantum dot subject to strong interactions, by providing an exact, nonperturbative formalism that allows us to carry out a systematic analysis of the thermopower at any frequency. Special emphasis is put on the dc and high-frequency limits. We demonstrate that, in the Kondo regime, the ac thermopower is characterized by a universal function that we determine numerically.

PACS numbers: 72.15.Qm, 72.15.Jf, 73.63.Kv

I. INTRODUCTION

In the quest to find the most energy-efficient systems and devices, thermal generation of currents in nanometer-size structures which can be manipulated by electric fields, may offer one of the best paths to follow.¹⁻³ Quantum dots (QD) are among the best candidates, since they are highly tunable. Moreover, they are characterized by an enhanced figure of merit, as a result of the converging effect of reduced spatial dimensionality, that minimizes the phonon thermal conductivity, and an increased electronic density of states. So far, they can be used as thermoelectric power generators or coolers⁴, and when embedded into bulk materials or nanowires, a structure with large thermopower coefficient, S , is obtained.^{5,6} The same environment, however, is fundamentally enhancing the interaction between the electrons, generating strong correlations and other dynamical effects. By doing detailed measurements in QDs, it has been shown that the oscillating behavior of the thermopower as a function of the gate voltage might carry information on interactions present in the system.⁷ On the theoretical side, the thermoelectric problem in quantum dots is also of considerable interest: First, a perturbative calculation valid for weakly interacting QDs was presented in Ref. 8. Later on, in Refs. 9 and 10 the thermopower of a Kondo correlated dot was computed. Quite recently, by using the numerical renormalization group approach (NRG) approach, the thermoelectric properties of a strongly correlated dot modeled in terms of the Anderson model, were investigated systematically.¹¹ Other more exotic systems such as the SU(4) Kondo state¹² or double-dot systems¹³ were also studied, but, so far, mostly static effects have been addressed¹⁴ and only few theoretical and experimental studies were focused on dynamical effects.¹⁵ In contrast, other transport quantities, such as the usual differential conductance or the noise, have been investigated at various frequencies.¹⁶⁻¹⁸ Consequently, new interesting physics has emerged: It was found that the modulation of the gate voltages suppresses the Kondo temperature¹⁹ T_K , and that the frequency-dependent emission noise of a quantum dot²⁰ in the Kondo regime, at high frequen-

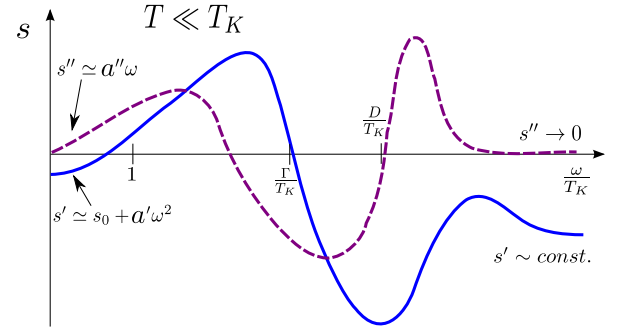


FIG. 1. (Color online) Sketch of the real and imaginary parts of the universal function $s(\omega/T_K, T/T_K)$ in the Kondo regime, at a fixed temperature, $T \ll T_K$. The coefficients a' and a'' depend on temperature as $\sim 1/T^2$. See also Eq. (21) for the functional dependence of s .

cies, $\hbar\omega \gg k_B T_K$, provides information on the system at energy scales which are not accessible by simple dc measurements. Furthermore, in a slightly different context, i.e., the correlated band models, it has been predicted that the thermopower in the high-frequency limit may provide further understanding on the thermoelectric transport.²¹⁻²³

Motivated by these observations, we consider here the problem of thermoelectric response at finite frequencies in a quantum dot subject to a strong Coulomb interaction, and in particular we shall investigate the dynamical thermopower $S(\omega)$. This quantity characterizes how a charge current, $I^{(1)}(t)$, is generated by an infinitesimal time-dependent temperature difference $\delta T(t)$ across the dot and, at the same time, how a heat current $I^{(2)}(t)$ responds to an infinitesimal voltage drop $\delta V(t)$ ²⁴

$$\begin{pmatrix} \langle I^{(1)}(t) \rangle \\ \langle I^{(2)}(t) \rangle \end{pmatrix} = \int dt' dt'' T S(t-t') G(t'-t'') \times \begin{pmatrix} \delta T(t'')/T|_{\delta V=0} \\ \delta V(t'')|_{\delta T=0} \end{pmatrix}. \quad (1)$$

As defined, the thermopower itself is not a response function, so it can not be computed directly within the linear response theory. Instead, the combination $L_{12}(\omega) =$

$TG(\omega)S(\omega)$ that appears in Eq. (1) is a true response function that can be computed exactly. To get the thermopower spectrum $S(\omega)$, aside from L_{12} we also need the usual ac conductance, $G(\omega) = L_{11}(\omega)$. Then, $S(\omega)$ can be expressed as^{22,25}

$$S(\omega) = \frac{1}{T} \left\{ \frac{L_{12}(\omega)}{L_{11}(\omega)} \right\}. \quad (2)$$

One of the main results of this work is that in the strong coupling (Kondo) regime, i.e., $\max\{\omega, T\} \ll T_K$, the equilibrium ac thermopower takes on a simple, universal form, which apart from a phase-dependent prefactor, is characterized by a universal function

$$S(\omega, T) \simeq \frac{k_B}{e} \left(\frac{T}{T_K} \right) s(\omega/T_K, T/T_K) \cot(\delta_0). \quad (3)$$

Here, δ_0 is the phase shift of the electrons at the Fermi level, and the function s is a complex universal function that depends exclusively on ω/T_K and T/T_K . The prefactor $k_B/e = 8.6 \times 10^{-5}$ V/K is the unit in which the thermopower is measured. The characteristic features of $s(\omega/T_K, T/T_K)$ are sketched in Fig. 1. At a given temperature $T \ll T_K$, and when $\omega \ll T_K$, the real part s' grows quadratically with the frequency $s' \simeq s_0 + a'(T)\omega^2 + \dots$, followed by multiple changes of sign at some intermediate frequencies, $\omega_i \sim \{T, \Gamma\}$, and becomes constant in the $\omega \rightarrow \infty$ limit. Its imaginary part vanishes in the $\omega \rightarrow 0$ limit, has a linear dependence $s'' \simeq a''(T)\omega + \dots$ below the Kondo scale, and vanishes in the $\omega \rightarrow \infty$ limit.

In Fig. 2, we present a sketch of the setup. It consists of a quantum dot that is coupled to two external leads, $\alpha = \{L, R\}$, that have different temperatures, $T_\alpha(t) = T \pm \delta T(t)/2$. The temperature gradient $\delta T(t)$ generates a time-dependent current which flows across the dot. Starting from the Kubo formalism and Fourier transforming from time t to frequency ω , we find the ac thermopower, $S(\omega)$. We derive general, exact expressions for $L_{ij}(\omega)$, and implicitly for $S(\omega)$, which are valid at any frequency (see Eqs. (2) and (15)). The derivation is then followed by a careful analysis of different regimes of interest, such as the large-frequency limit, $S^* = S(\omega \rightarrow \infty)$, or the conventional low-frequency limit, $S_0 = S(\omega = 0)$ ¹¹. As a technical observation, since we are interested in $S(\omega)$ at any frequency, even in the region $\omega \gg D$, the bandwidth D of the conduction electrons must be kept finite in the calculations, otherwise an unphysical divergence with increasing frequency is present in the spectrum of $L_{12}(\omega)$ (see Sec. III).

The paper is organized as follows: In Sec. II, we introduce the model Hamiltonian and derive the exact expressions for the generalized susceptibilities $L_{ij}(\omega)$ that enter Eq. (2). The operators for the charge and heat currents are discussed in Sec. II B, and the results for the ac thermopower are presented in Sec. III. We give the final remarks in Sec. IV. Further technical details are discussed in Appendices A and B.

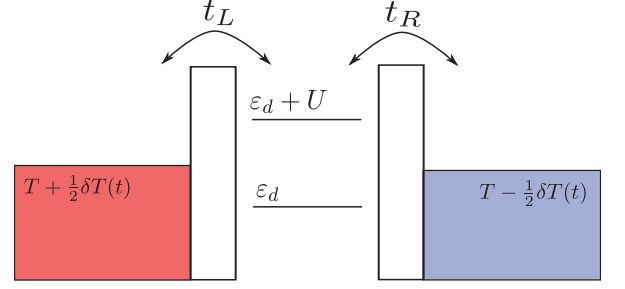


FIG. 2. (Color online) Sketch of the quantum dot that is coupled to two external leads which are assumed to be at different temperatures $T \pm \delta T(t)/2$.

II. THEORETICAL FRAMEWORK

A. Model Hamiltonian

In this work, we shall consider the case of a QD described by the Anderson model. It consists of a single localized orbital that is coupled to two external leads (see Fig. 2). The dot can accommodate up to two electrons with strong on-site interaction. The Hamiltonian takes the form

$$H = \sum_{\sigma} \epsilon_d d_{\sigma}^{\dagger} d_{\sigma} + U d_{\uparrow}^{\dagger} d_{\uparrow} d_{\downarrow}^{\dagger} d_{\downarrow} + \sum_{\mathbf{k}, \sigma} \sum_{\alpha=L,R} \left(\epsilon_{\mathbf{k}} c_{\alpha \mathbf{k} \sigma}^{\dagger} c_{\alpha \mathbf{k} \sigma} + \left(t_{\alpha \mathbf{k}} c_{\alpha \mathbf{k} \sigma}^{\dagger} d_{\sigma} + H.c. \right) \right), \quad (4)$$

where d_{σ} is the annihilation operator of an electron with spin σ in the dot, and $c_{\alpha \mathbf{k} \sigma}^{\dagger}$ is the creation operator of an electron with momentum \mathbf{k} and spin σ in lead $\alpha = \{L, R\}$. They satisfy the usual anticommutation relations: $\{d_{\sigma}, d_{\sigma'}^{\dagger}\} = \delta_{\sigma\sigma'}$ and $\{c_{\alpha \mathbf{k} \sigma}, c_{\alpha' \mathbf{k}' \sigma'}^{\dagger}\} = (2\pi)^3 \delta(\mathbf{k} - \mathbf{k}') \delta_{\alpha\alpha'} \delta_{\sigma\sigma'}$. We treat the leads as having a constant density of states $\varrho(\omega) = \varrho_0 = 1/(2D)$, with $2D$ the bandwidth. The tunneling matrix is considered as being momentum independent, $t_{\alpha \mathbf{k}} = t_{\alpha}$. Its strength is characterized by the usual hybridization function $\Gamma_{\alpha} = \pi \varrho_0 t_{\alpha}^2$. We define the total hybridization as $\Gamma = \sum_{\alpha=\{L,R\}} \Gamma_{\alpha}$. The dot itself supports a single orbital with energy ϵ_d subject to the on-site Coulomb interaction U . Close to the electron-hole symmetric configuration, $\epsilon_d \simeq -U/2$, the dot is in the Kondo regime, characterized by the Kondo energy scale which is defined as²⁶

$$T_K = \sqrt{\frac{U\Gamma}{4}} e^{\pi \epsilon_d (\epsilon_d + U)/\Gamma U}. \quad (5)$$

B. Currents and response functions

To compute the response functions, we need to define the charge and the heat currents. We introduce first the

charge- and heat-transfer operators

$$\begin{aligned} Q_\alpha &= Q_\alpha^{(1)} = e \sum_{\mathbf{k}, \sigma} c_{\alpha\mathbf{k}\sigma}^\dagger c_{\alpha\mathbf{k}\sigma}, \\ K_\alpha &= Q_\alpha^{(2)} = \sum_{\mathbf{k}, \sigma} (\varepsilon_{\mathbf{k}} - \mu_\alpha) c_{\alpha\mathbf{k}\sigma}^\dagger c_{\alpha\mathbf{k}\sigma}, \end{aligned} \quad (6)$$

and define the currents as time derivatives of the corresponding charge/heat operators:

$$I_\alpha^{(i)} = (-1)^{i+1} \frac{dQ_\alpha^{(i)}}{dt}. \quad (7)$$

Their explicit expressions can be obtained in terms of the equations of motion as:

$$\begin{aligned} I_\alpha^{(1)} &= i \frac{e}{\hbar} \sum_{\mathbf{k}, \sigma} t_\alpha c_{\alpha\mathbf{k}\sigma}^\dagger d_\sigma + H.c., \\ I_\alpha^{(2)} &= -\frac{i}{\hbar} \sum_{\mathbf{k}, \sigma} (\varepsilon_{\mathbf{k}} - \mu_\alpha) t_\alpha c_{\alpha\mathbf{k}\sigma}^\dagger d_\sigma + H.c.. \end{aligned} \quad (8)$$

To avoid a two-channel calculations, it is customary to perform a rotation of the L/R basis to a new one $\{\alpha_{\mathbf{k}\sigma}, \tilde{\alpha}_{\mathbf{k}\sigma}\}$, defined by: $\alpha_{\mathbf{k}\sigma} = \xi_L c_{L\mathbf{k}\sigma} + \xi_R c_{R\mathbf{k}\sigma}$ and $\tilde{\alpha}_{\mathbf{k}\sigma} = \xi_R c_{L\mathbf{k}\sigma} - \xi_L c_{R\mathbf{k}\sigma}$. This unitary transformation decouples the odd channel, $\tilde{\alpha}_{\mathbf{k}\sigma}$, from the dot, so that the dot remains coupled only to the even channel, $\alpha_{\mathbf{k}\sigma}$. The coefficients are $\xi_\alpha = t_\alpha / \sqrt{t_L^2 + t_R^2}$ and satisfy $\xi_L^2 + \xi_R^2 = 1$. Following this unitary transformation, only the interacting part of the Hamiltonian H_{int} changes to $H_{\text{int}} = t_{\text{eff}} \sum_{\mathbf{k}, \sigma} \alpha_{\mathbf{k}\sigma}^\dagger d_\sigma + h.c.$, with $t_{\text{eff}} = \sqrt{t_L^2 + t_R^2}$. In what follows we shall consider the perfectly symmetric dot, $t_L = t_R = t$. The currents, $I^{(i)} = (I_L^{(i)} - I_R^{(i)})/2$, transform accordingly, and under equilibrium conditions, $\mu_{L/R} = 0$, in the new basis they are defined as:

$$I^{(1)} = i \frac{e t_{\text{eff}}}{2\sqrt{2}\hbar} \sum_{\mathbf{k}, \sigma} \tilde{\alpha}_{\mathbf{k}\sigma}^\dagger d_\sigma + H.c. \quad (9)$$

$$I^{(2)} = -i \frac{t_{\text{eff}}}{2\sqrt{2}\hbar} \sum_{\mathbf{k}, \sigma} \varepsilon_{\mathbf{k}} \left(\tilde{\alpha}_{\mathbf{k}\sigma}^\dagger d_\sigma + H.c. \right), \quad (10)$$

and are expressed in terms of the decoupled channel operators only. This allows us to obtain exact results for the response functions. The currents $I_{L/R}^{(i)}$ also have a symmetrical component, which gets subtracted out in the definition of $I^{(i)}$. Within the Kubo formalism, the generalized response functions L_{ij} are given by²⁷

$$L_{ij}(t, t') = -\frac{i}{\hbar} \Theta(t - t') \langle [I^{(i)}(t), Q^{(j)}(t')] \rangle, \quad (11)$$

where

$$Q^{(i)} = \frac{Q_L^{(i)} - Q_R^{(i)}}{2}. \quad (12)$$

We want to express L_{ij} in terms of locally defined operators only, and for that we eliminate the charge operators. In Fourier space we obtain

$$L_{ij}(\omega) = -\frac{T_{ij}(\omega) - T_{ij}(0)}{i\omega}, \quad (13)$$

with $T_{ij}(\omega)$ the Fourier transform of the generalized susceptibility:

$$T_{ij}(t, t') = -\frac{i}{\hbar} \Theta(t - t') \langle [I^{(i)}(t), I^{(j)}(t')] \rangle. \quad (14)$$

Somewhat similar to the calculation of the ac conductance¹⁶, the calculation of thermopower, $S(\omega) = S'(\omega) + S''(\omega)$, reduces to the calculation of $A_d(\omega) = -\text{Im} G_d^R(\omega)/\pi$ - the spectral representation of the d-level operators in the dot (see Appendix B). In the present work $A_d(\omega)$ shall be computed by using the Wilson numerical renormalization group approach²⁸⁻³⁰ (NRG) as implemented in the Flexible-NRG code.³¹ Throughout the NRG calculation, the Wilson ratio was fixed to $\Lambda = 2$, and we have kept on average 4000 multiplets at each iteration.

III. AC THERMOPOWER

Let us now focus on the calculations of the response functions L_{ij} and the ac thermopower $S(\omega)$. In general, $L_{ij}(\omega)$ are complex functions of ω , as their imaginary parts capture retardation effects due to the external excitation. The full ω dependence of the $\text{Re} L_{ij}(\omega)$ acquires a relatively compact expression in terms of the spectral representation of the d-level:

$$\begin{aligned} \text{Re} L_{ij}(\omega) &= \frac{t_{\text{eff}}^2}{2\omega\hbar} \left(-\frac{e}{\hbar} \right)^{4-i-j} \varrho_0 \int d\omega' \{ \text{Im} G_d^R(\omega') \\ &\quad [(\omega' - \omega)^{i+j-2} \Theta_{\omega' - \omega} f(\omega' - \omega) + \\ &\quad + (\omega' + \omega)^{i+j-2} \Theta_{\omega' + \omega} f(\omega') - \\ &\quad - (\omega' - \omega)^{i+j-2} \Theta_{\omega' - \omega} f(\omega') \\ &\quad - (\omega' + \omega)^{i+j-2} \Theta_{\omega' + \omega} f(\omega' + \omega)] \}, \end{aligned} \quad (15)$$

with $\Theta_\omega = \Theta(D - |\omega|)$ and $f(\omega)$ the Fermi-Dirac distribution. To get the ac conductance¹⁶, the high energy cut-off D can be safely taken to infinity, as L_{11} remains a regular function. This is not the case for L_{12} which diverges at large frequencies when $D \rightarrow \infty$, so it is compulsory to have a finite bandwidth for the conduction electrons. To get the imaginary part of L_{ij} , the use of the Hilbert transform is unavoidable. We first compute $\text{Re} L_{ij}$, and then $\text{Im} L_{ij}$ is obtained by a Kramers-Krönig(KK) transformation

$$\text{Im} L_{ij}(\omega) = -\frac{1}{\pi} \int_{-\infty}^{+\infty} \frac{\text{Re} L_{ij}(\omega')}{\omega' - \omega} d\omega' \quad (16)$$

Although Eq. (15) looks cumbersome, we can interpret it in terms of inelastic tunneling processes and see these correlation functions as rates by which the system absorbs or emits photons²⁰ at frequencies ω . Further details on how to compute L_{ij} are presented in Appendix B. With L_{ij} at hand, $S(\omega)$ can be obtained by using Eq. (2). By symmetry, $S'(\omega) = S'(-\omega)$, is an even function of frequency,

while $S''(\omega) = -S''(-\omega)$, is an odd function. The full ω and T dependence for $S(\omega)$ is displayed in Figs. 3(a)-3(f), while in Figs. 3(g) and 3(h) a cut at constant temperature $T = 0.1\Gamma$ is presented. In Figs. 3(a)-3(b),

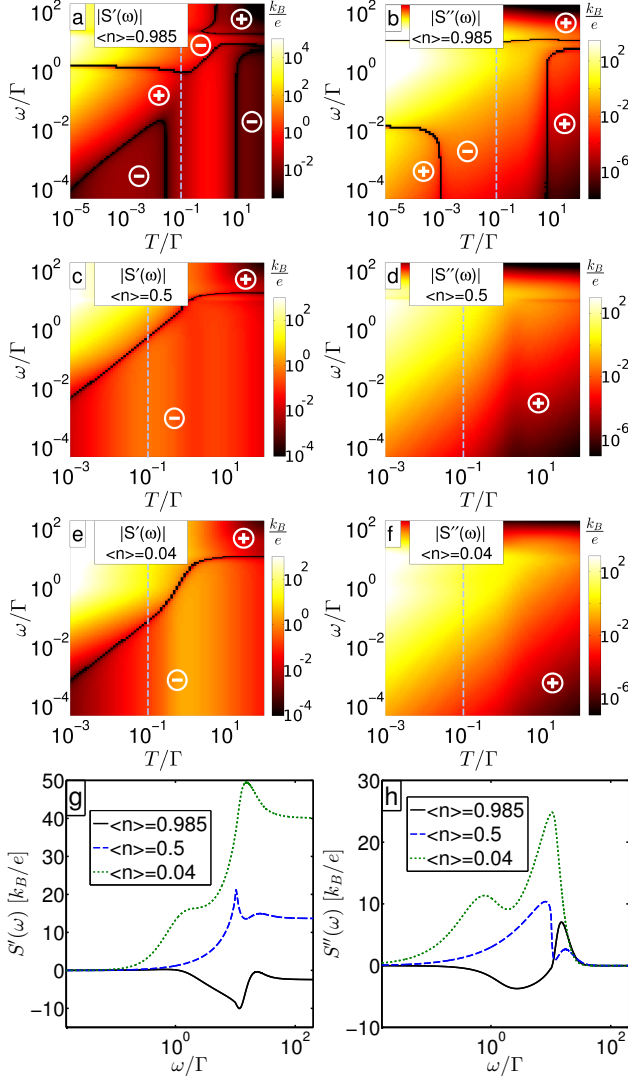


FIG. 3. (Color online) Density plots for the real and imaginary parts of the thermopower in the (T, ω) plane: (a), (b) Kondo regime, (c), (d) mixed valence regime, and (e), (f) empty orbital regime. Panels (g) and (h) represent the thermopower at $T = 0.1\Gamma$ for positive ω along the dashed lines in the density plots. The darker lines are the locations of the zeros, and mark the positions where the thermopower changes sign. The (\pm) symbols indicate the signs of $S(\omega)$. The NRG parameters used are $U/\Gamma = 10$, $\varepsilon_d/\Gamma = -4$ ($n = 0.985$), $\varepsilon_d/\Gamma = -0.2$ ($n = 0.5$) and $\varepsilon_d/\Gamma = 5$ ($n = 0.04$).

we represent the results for $S(\omega, T)$ when the system is in the Kondo regime, where $\varepsilon_d \simeq -U/2$, and $\langle n \rangle \simeq 1$. Figs. 3(c) and 3(d) present results for $S(\omega, T)$ in the mixed valence regime with $\langle n \rangle = 0.5$, while Figs. 3(e) and 3(f) show $S(\omega, T)$ in the empty orbital limit, $\langle n \rangle \ll 1$. By symmetry, when $1 < n < 2$, the thermopower has the same magnitude, but opposite sign, as the role of parti-

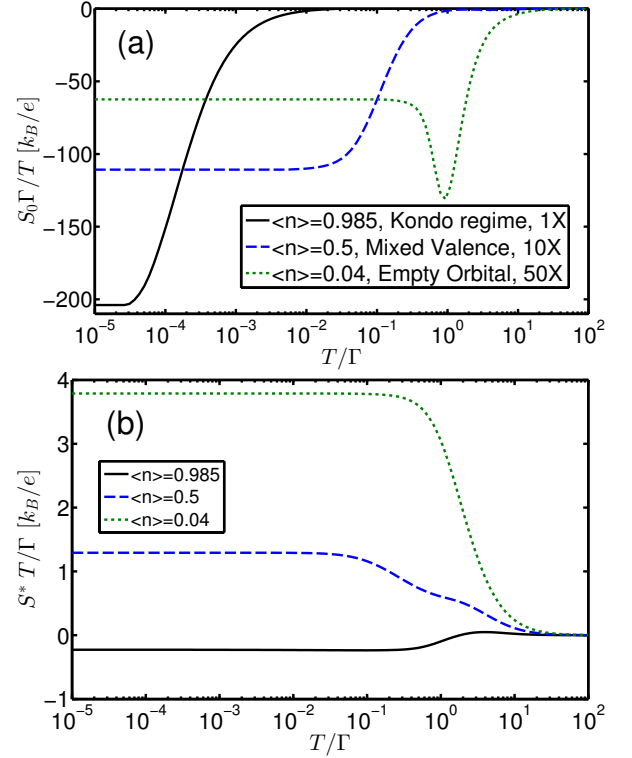


FIG. 4. (Color online) (a) The dc-thermopower $S_0 = S(\omega = 0)$ as function of temperature in different regimes. (b) Temperature dependence of $S^* = S(\omega \gg D)$.

cles and holes is inverted. At the electron-hole symmetric point, i.e., $n = 1$, the particles and holes move together in the same direction under the temperature gradient, and the thermopower vanishes exactly.

At very small frequencies and temperatures, $\{\omega, T\} \rightarrow 0$, only the quasiparticles very close to the Fermi surface give a contribution to the currents flowing through the device, so this limit can be understood in terms of the Fermi-liquid picture.³² The Fermi-liquid scale Ω_F , is controlled by either T_K within the Kondo regime, or by Γ itself otherwise. When $\{\omega, T\} \ll \Omega_F$, the frequency dependence of $S(\omega)$ is captured by a simple analytical expression

$$S(\omega, T) = S_0(T) + b'(T)\omega^2 + i b''(T)\omega + \dots \quad (17)$$

Here $S_0(T) < 0$, is the dc-thermopower, while b' and b'' are some coefficients that depend on temperature. In the Kondo regime, $\{b'(T), b''(T)\} \sim 1/T$. In our convention, positive (negative) S_0 corresponds to the situation when charge and heat currents flow in the same (opposite) directions. At some intermediate frequencies, $\omega \sim T$, $S'(\omega)$ changes sign and becomes positive. In the Kondo regime, there is another change of sign at a larger, almost constant frequency $\omega_2 \simeq \Gamma$, and S' becomes negative in the $\omega \gg D$ limit. The sign of $S_0(T)$ can be associated with the type of dominant carriers in the system at that particular energy: hole like carriers correspond to $S_0 > 0$, and particle like carriers to $S_0 < 0$. The first sign change

in $S_0(T)$ can be understood as follows: At $T \simeq 0$, the Kondo peak is weighted towards positive energies (for $n < 1$), but as temperature increases, it is pulled towards the negative energy region. Thus, the quantum dot shifts from having predominantly particle carriers, to having predominantly hole carriers in the window $\sim T$ that contributes to the transport. Whenever the average entropy carried inside this window becomes zero, the thermopower vanishes. At a finite frequency ω , inelastic tunneling processes in a window $\sim 2\omega$ around the Fermi level give additional contributions to the transport, see Eq. (15). The picture gets more complicated by the existence of retardation effects, which lead to finite imaginary parts in the response functions, and consequently affect the zeros of the thermopower. The high-frequency features in Fig. 3 at energies $\omega \sim \{U, D\}$ can be associated with Hubbard charging, and eventually band-edge effects. In Fig. 4, we display the temperature dependence of $S_0(T)$ and $S^*(T)$. It has been already shown³³ that in the Kondo regime, when $T \ll T_K$, S_0 depends linearly on T , $S_0 \propto T$. This observation carries over to the mixed valence and empty orbital regimes too, as long as $T \ll \Gamma$. In the opposite limit, $T \gg T_K$, S_0 shows a change of sign at some large temperature, and then decays towards zero.

In the large-frequency limit $\omega \gg D$, S^* can be evaluated simply as

$$S^*(T) = \frac{1}{T} \frac{L_{12}^*}{L_{11}^*}. \quad (18)$$

with L_{ij}^* some temperature-dependent coefficients, discussed in Appendix B (see Eq. (B6)). As $\omega \gg D$, all states are involved in transport, so that the only energy scale that survives is the bandwidth itself (as long as $\{T_K, U\} \ll D$). Therefore, we expect the features of $S^*(T)$ to carry information only on D itself. In the small-temperature limit, $T \rightarrow 0$, the L_{ij}^* 's become constants, so a divergent behavior $S^* \propto 1/T$ emerges in this limit. This is clearly visible in Fig. 4 (b), where S^*T becomes constant when $T \ll \Gamma$. At intermediate temperatures, $\Gamma < T < D$, S^* decreases significantly, and vanishes in the large T limit.

In what follows we shall focus on the strongly correlated regime. When $\{\omega, T\} \leq T_K$, a clear universal behavior emerges as $S(\omega)$ depends exclusively on the T/T_K and ω/T_K ratios. It was found previously¹¹ that as long as $T \ll T_K$,

$$\begin{aligned} s_0(T/T_K) &= \left(\frac{e}{\pi\gamma T} \right) S_0(T) \tan \delta_0 \\ &= \frac{e}{k_B} \left(\frac{T_K}{T} \right) S_0(T) \left(\frac{\tan \delta_0}{\tilde{\gamma}} \right) \end{aligned} \quad (19)$$

is a universal function that scales with T/T_K up to a filling-dependent phase factor. Here, δ_0 is the phase shift at the Fermi level, $\delta_0 = \pi\langle n \rangle/2$, with $\langle n \rangle$ the average occupation of the dot, γ is the specific-heat coefficient of the quantum dot which is filling dependent, and $\tilde{\gamma} = \pi\gamma T_K/k_B$ is a dimensionless quantity of the order 1. In

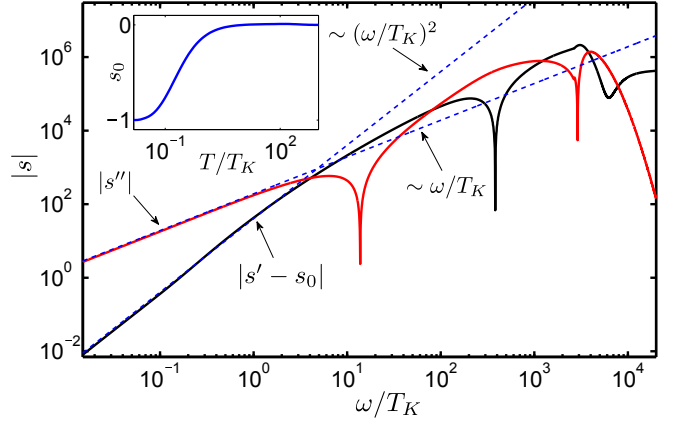


FIG. 5. (Color online) Universal scaling functions for a filling $\langle n \rangle = 0.95$ for a fixed temperature, $T = 0.02 T_K$. In the inset, we represent the s_0 universal function.

the inset of Fig. 5 we represent $s_0(T/T_K)$ as a function of T/T_K for a filling $\langle n \rangle = 0.95$. We extend this analysis to finite frequencies where a similar behavior emerges, as the ac thermopower can be expressed as:

$$S(\omega, T) = \frac{k_B}{e} \left(\frac{T}{T_K} \right) s(\omega/T_K, T/T_K) \tilde{\gamma} \cot(\delta_0). \quad (20)$$

The universal scaling function s depends on ω/T_K and T/T_K only. A sketch with the frequency dependence is presented in Fig. 1, while in Fig. 5 we represent the exact numerical calculation for the frequency dependence of $|s|$. In the Fermi-liquid regime, $\{\omega, T\} \ll T_K$, simple analytical expressions can approximate the real and imaginary parts of s :

$$\begin{aligned} s' \left(\frac{\omega}{T_K}, \frac{T}{T_K} \right) &= s_0 \left(\frac{T}{T_K} \right) + \alpha' \left(\frac{\omega}{T_K} \right)^2 \left(\frac{T_K}{T} \right)^2 + \dots, \\ s'' \left(\frac{\omega}{T_K}, \frac{T}{T_K} \right) &= \alpha'' \left(\frac{\omega}{T_K} \right) \left(\frac{T_K}{T} \right)^2 + \dots \end{aligned} \quad (21)$$

with α' and α'' some coefficients ~ 1 . The $s' \sim \omega^2$ frequency dependence can be related to the virtual Kondo transitions from the singlet ground state to the excited states.³⁴ These transitions give for the imaginary part of the T-matrix: $\text{Im } T(\omega, T) \propto 1 - (3\omega^2 + \pi^2 T^2)/T_K^2$, when $\{\omega, T\} \ll T_K$, which in turn introduces corrections of the order $\sim \omega^2$ and $\sim T^2$ in the response functions $\text{Re } L_{ij}$. Simple analytics then show that $s' \sim \omega^2/T^2$. Then, by Hilbert transform, s'' is linear in frequency. This scaling for s extends up to frequencies of the order of $\omega \sim T_K$, followed by a sign change at some particular frequencies ω_i . At very large frequencies $\omega \gg T_K$, s' becomes a constant, while $s'' \rightarrow 0$.

IV. CONCLUDING REMARKS

We have studied the finite-frequency thermopower of a quantum dot described by the Anderson model. For that

we have first constructed a general framework which allowed us to investigate in a non-perturbative manner the ac thermopower. When calculating the ac conductance¹⁶, it is safe to take the bandwidth $D \rightarrow \infty$, but when we address the problem of the ac thermopower, it is compulsory to keep D finite. Although $S(\omega)$ presents a relatively rich structure that includes several sign changes, in the Fermi liquid regime a simple analytical expression is able to capture its behavior over a broad range of temperatures and frequencies. In the Kondo regime, the ac thermopower is characterized by a universal function that we have determined numerically. We have also found that the S_0 and S^* have a markedly different behavior in the low-temperature limit.

ACKNOWLEDGMENTS

We would like to thank I. Weymann for carefully reading our manuscript. This research has been financially supported by UEFISCDI under French-Romanian Grant DYMESYS (PN-II-ID-JRP-2011-1 and ANR 2011-IS04-001-01) and by Hungarian Research Funds under grant Nos. K105149, CNK80991, TAMOP-4.2.1/B-09/1/KMR-2010-0002.

Appendix A: Green's Functions

Within the L/R basis transformation, one channel becomes decoupled, and can be treated as a non-interacting one. It is simply described by the non-interacting Hamiltonian $H_0 = \sum_{\mathbf{k},\sigma} \varepsilon_{\mathbf{k}} \tilde{\alpha}_{\mathbf{k}\sigma}^\dagger \tilde{\alpha}_{\mathbf{k}\sigma}$. In what follows, we shall fix the chemical potential to zero. The non-equilibrium evolution of the system is described by the conduction electron Green's function: $g_{\mathbf{k}\sigma}(t - t') = -i\langle \mathcal{T}_C \tilde{\alpha}_{\mathbf{k}\sigma}(t) \tilde{\alpha}_{\mathbf{k}\sigma}^\dagger(t') \rangle$, where \mathcal{T}_C is the time ordering operator on the Keldysh contour. Within this language, we can define four Green's functions. Two combinations define the greater and lesser components

$$\begin{aligned} g_{\mathbf{k}\sigma}^>(t - t') &= -i\langle \tilde{\alpha}_{\mathbf{k}\sigma}(t) \tilde{\alpha}_{\mathbf{k}\sigma}^\dagger(t') \rangle, \\ g_{\mathbf{k}\sigma}^<(t - t') &= i\langle \tilde{\alpha}_{\mathbf{k}\sigma}^\dagger(t') \tilde{\alpha}_{\mathbf{k}\sigma}(t) \rangle, \end{aligned} \quad (\text{A1})$$

while the other two define the time and anti-time ordered ones: $g_{\mathbf{k}\sigma}^t(t - t') = -i\langle \mathcal{T} \tilde{\alpha}_{\mathbf{k}\sigma}(t) \tilde{\alpha}_{\mathbf{k}\sigma}^\dagger(t') \rangle$, and $g_{\mathbf{k}\sigma}^{\bar{t}}(t - t') = -i\langle \tilde{\mathcal{T}} \tilde{\alpha}_{\mathbf{k}\sigma}(t) \tilde{\alpha}_{\mathbf{k}\sigma}^\dagger(t') \rangle$. Here \mathcal{T} and $\tilde{\mathcal{T}}$ are the time and anti-time ordering operators. We also introduce the retarded and the advanced Green's functions, which are defined in the usual way:

$$\begin{aligned} g_{\mathbf{k}\sigma}^A(t - t') &= i\Theta(t' - t)\langle \{\tilde{\alpha}_{\mathbf{k}\sigma}(t), \tilde{\alpha}_{\mathbf{k}\sigma}^\dagger(t')\} \rangle, \\ g_{\mathbf{k}\sigma}^R(t - t') &= -i\Theta(t - t')\langle \{\tilde{\alpha}_{\mathbf{k}\sigma}(t), \tilde{\alpha}_{\mathbf{k}\sigma}^\dagger(t')\} \rangle. \end{aligned} \quad (\text{A2})$$

We are interested in the momentum integrated Green's function $g_\sigma(\omega) = \sum_{\mathbf{k}} g_{\mathbf{k}\sigma}(\omega)$, as these are the only quantities that explicitly enter the expression for the ac thermopower. Here, we consider the simplest situation

of a dispersionless electronic band with a band cutoff D . It is characterized by a constant density of states $N(\omega) = 1/(2D)\Theta(D - |\omega|) = N(0)\Theta_\omega$, with $N(0) = 1/(2D)$, the DOS at the Fermi level and $\Theta_\omega = \Theta(D - |\omega|)$. Then, the momentum integrated Green's function have relatively simple analytical expressions³⁵: $g_\sigma^>(\omega) = -2\pi i(1 - f(\omega))N(0)\Theta_\omega$, $g_\sigma^<(\omega) = 2\pi i f(\omega)N(0)\Theta_\omega$ and $\text{Im} g_\sigma^A(\omega) = -\text{Im} g_\sigma^R(\omega) = i\pi N(0)\Theta_\omega$. Usually, $\text{Re} g^{R/A}$ is neglected in the large-bandwidth limit, but as long as we are interested in the response functions L_{ij} in the large $\omega > D$ limit, its contribution becomes important.

Appendix B: Current Correlations and the dynamical transport coefficients

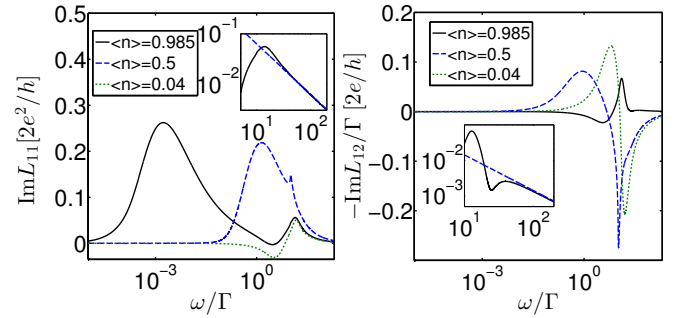


FIG. 6. (Color online) The imaginary part of the dynamical coefficients $L_{ij}(\omega)$ as function of frequency. The inset shows the asymptotic $\sim 1/\omega$ behavior in the large- ω limit in the Kondo regime for $\langle n \rangle = 0.985$. The temperature was fixed to $T=10^{-5}\Gamma$.

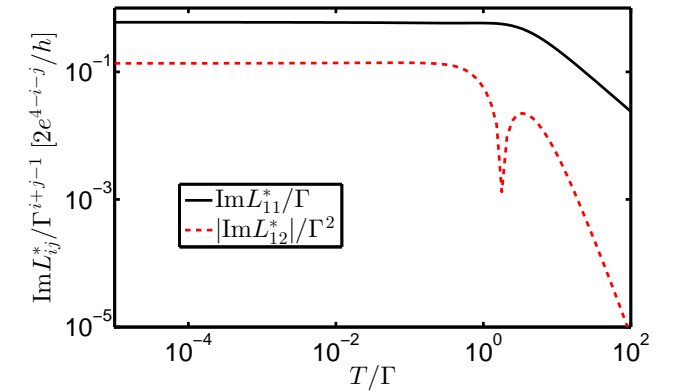


FIG. 7. (Color online) The temperature dependence of L_{ij}^* in the Kondo regime. The results are obtained by using the sum rule expression, Eq. (B6).

To get the dynamical transport coefficients, we need to compute the retarded response functions defined in Eq. (14), with the current operators defined in Eqs. (9) and (10). In the even/odd basis, one channel becomes decoupled and the charge current correlator T_{11} can be

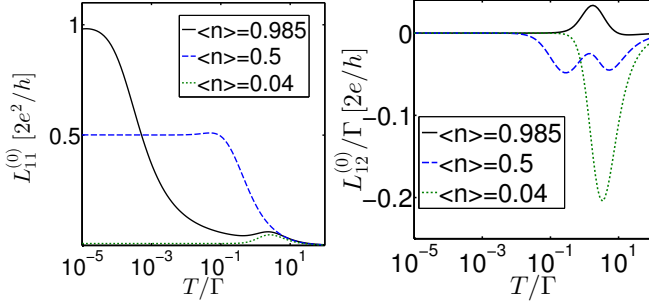


FIG. 8. (Color online). The temperature dependence of $\text{Re} L_{ij}^{(0)}$. Here $L_{11}^{(0)}$ can be identified with the dc-conductance itself.

evaluated as:

$$T_{11}(t-t') = \Theta(t-t') \frac{e^2}{\hbar^3} \frac{t_{\text{eff}}^2}{4} \sum_{\mathbf{k}, \sigma} \{ G_d^>(t-t') g_{\mathbf{k}\sigma}^<(t'-t) - G_d^<(t-t') g_{\mathbf{k}\sigma}^>(t'-t) - G_d^<(t'-t) g_{\mathbf{k}\sigma}^>(t-t') - G_d^>(t'-t) g_{\mathbf{k}\sigma}^<(t-t') \}, \quad (\text{B1})$$

which gives for L_{11} defined in Eq. (13) a relatively compact expression:

$$\text{Re} L_{11}(\omega) = -\frac{t_{\text{eff}}^2}{2\omega} \frac{e^2}{\hbar^3} \varrho_0 \int d\omega' \{ \text{Im} G_d^R(\omega') [\Theta_{\omega'-\omega} f(\omega'-\omega) + \Theta_{\omega'+\omega} f(\omega') - \Theta_{\omega'-\omega} f(\omega') - \Theta_{\omega'+\omega} f(\omega'+\omega)] \}. \quad (\text{B2})$$

Notice that within the present formalism, we can identify $\text{Re} L_{11}(\omega)$ with the real part of the ac conductance $G(\omega)$.¹⁶ A similar expression can be derived for $T_{12}(t, t')$, which in the Fourier space becomes:

$$T_{12}(\omega) = -\frac{t_{\text{eff}}^2}{4} \frac{e}{\hbar^3} \sum_{\mathbf{k}, \sigma} \varepsilon_{\mathbf{k}} \int \frac{d\omega'}{2\pi} \{ G_d^R(\omega + \omega') g_{\mathbf{k}\sigma}^<(\omega') + G_d^<(\omega + \omega') g_{\mathbf{k}\sigma}^A(\omega') + G_d^>(\omega') g_{\mathbf{k}\sigma}^R(\omega + \omega') + G_d^A(\omega') g_{\mathbf{k}\sigma}^>(\omega + \omega') \}. \quad (\text{B3})$$

Subtracting the $T_{12}(\omega = 0)$ term and dividing by $-i\omega$, the real part of L_{12} is obtained as:

$$\text{Re} L_{12}(\omega) = \frac{t_{\text{eff}}^2}{2\omega} \frac{e}{\hbar^2} \varrho_0 \int d\omega' \{ \text{Im} G_d^R(\omega') [(\omega' - \omega) \Theta_{\omega'-\omega} f(\omega' - \omega) + (\omega' + \omega) \Theta_{\omega'+\omega} f(\omega') - (\omega' - \omega) \Theta_{\omega'-\omega} f(\omega') - (\omega' + \omega) \Theta_{\omega'+\omega} f(\omega' + \omega)] \}. \quad (\text{B4})$$

In these expressions, L_{ij} depends explicitly on the retarded localized d-level Green's function $G_d^R(\omega)$. This quantity shall be computed exactly by using the NRG method. In this way, Eqs. (B) and (B) are the exact expressions for the real parts of the Onsager transport coefficients, and no approximation of any kind was used so far. The ac thermopower depends not only on the real, but also on the imaginary parts of L_{ij} . Actually their imaginary parts give the main contribution in the large-frequency limit. To obtain them, we use the Kramers-Krönig relations, Eq. (16). In the ac limit, when ω is the largest energy scale ($\omega \gg D$), we can simplify considerably the calculation by noticing that

$$\text{Im} L_{ij}(\omega) \simeq \frac{L_{ij}^*}{\omega} \quad (\text{B5})$$

with L_{ij}^* some coefficients,

$$L_{ij}^* = \frac{1}{\pi} \int_{-\infty}^{+\infty} \text{Re} L_{ij}(\omega') d\omega', \quad (\text{B6})$$

which are thus determined as the sum rule of dynamical quantities.²³ In Fig. 6 we represent the imaginary parts of L_{ij} in the Kondo regime, as computed by doing the KK transformations of Eq. (B) and (B). The insets display the large-frequency behavior, which indicates that our approximation, Eq. (B5), is indeed correct. The temperature dependence of L_{ij}^* is displayed in Fig. 7.

In the small-frequency limit, $\omega \rightarrow 0$, the calculation can be simplified again. Introducing the notation $\text{Re} L_{ij}^{(0)} = \text{Re} L_{ij}(\omega \rightarrow 0)$, we notice that Eqs. (B) and (B) reduce considerably to

$$\text{Re} L_{ij}^{(0)} = \frac{t_{\text{eff}}^2}{\hbar} \left(-\frac{e}{\hbar} \right)^{4-i-j} \varrho_0 \times \int d\tilde{\omega} \left(\tilde{\omega}^{i+j-2} \text{Im} G_d^R(\tilde{\omega}) \frac{\partial f(\tilde{\omega})}{\partial \tilde{\omega}} \right). \quad (\text{B7})$$

Here, $\text{Re} L_{11}^{(0)}$ is the dc-conductance itself. Its temperature dependence is displayed in Fig. 8. As expected in the $T \rightarrow 0$ limit, $\text{Re} L_{11}^{(0)}$ shows the usual Kondo behavior, as the system is close to the unitary limit. From Eqs. (B7) and (2) one can notice that the thermopower has the form of an average entropy $-\langle \epsilon - \mu \rangle / (eT)$ carried per particle/hole across the quantum dot. Thus, for the case of perfect particle-hole symmetry, the thermopower becomes zero. This form can also be used to justify the $1/T$ dependence of S^* (see Fig. 3).

* chirlarazvan@yahoo.com

¹ B. C. Sales, D. Mandrus, and R. K. Williams, *Science* **272**, 1325 (1996).

² G. J. Snyder and E. S. Toberer, *Nat. Mater.* **7**, 104 (2008).

³ J. P. Heremans, V. Jovovic, E. S. Toberer, A. Saramat, K. Kurosaki, A. Charoenphakdee, S. Yamanaka, and G. J.

- Snyder, *Science* **321**, 554 (2008).
- ⁴ T. E. Humphrey, R. Newbury, R. P. Taylor, and H. Linke, *Phys. Rev. Lett.* **89**, 116801 (2002).
 - ⁵ T. C. Harman, P. J. Taylor, M. P. Walsh, and B. E. LaForge, *Science* **297**, 2229 (2002).
 - ⁶ R. Y. Wang, J. P. Feser, J.-S. Lee, D. V. Talapin, R. Segalman, and A. Majumdar, *Nano Letters* **8**, 2283 (2008).
 - ⁷ S. F. Svensson, A. I. Persson, E. A. Hoffmann, N. Nakpathomkun, H. A. Nilsson, H. Q. Xu, L. Samuelson, and H. Linke, *New Journal of Physics* **14**, 033041 (2012).
 - ⁸ C. W. J. Beenakker and A. A. M. Staring, *Phys. Rev. B* **46**, 9667 (1992).
 - ⁹ D. Boese and R. Fazio, *Europhys. Lett.* **56**, 576 (2001).
 - ¹⁰ R. Scheibner, H. Buhmann, D. Reuter, M. N. Kiselev, and L. W. Molenkamp, *Phys. Rev. Lett.* **95**, 176602 (2005).
 - ¹¹ T. A. Costi and V. Zlatić, *Phys. Rev. B* **81**, 235127 (2010).
 - ¹² P. Roura-Bas, L. Tosi, A. A. Aligia, and P. S. Cornaglia, *Phys. Rev. B* **86**, 165106 (2012).
 - ¹³ P. Trocha and J. Barnaś, *Phys. Rev. B* **85**, 085408 (2012).
 - ¹⁴ S. Donsa, S. Andergassen, and K. Held, arXiv:1308.4882 (2013).
 - ¹⁵ J. S. Lim, R. López, and D. Sánchez, *Phys. Rev. B* **88**, 201304 (2013).
 - ¹⁶ M. Sindel, W. Hofstetter, J. von Delft, and M. Kindermann, *Phys. Rev. Lett.* **94**, 196602 (2005).
 - ¹⁷ Y. M. Blanter and E. V. Sukhorukov, *Phys. Rev. Lett.* **84**, 1280 (2000).
 - ¹⁸ C. P. Moca, I. Weymann, and G. Zarand, *Phys. Rev. B* **84**, 235441 (2011).
 - ¹⁹ A. Kogan, S. Amasha, and M. A. Kastner, *Science* **304**, 1293 (2004).
 - ²⁰ J. Basset, A. Y. Kasumov, C. P. Moca, G. Zaránd, P. Simon, H. Bouchiat, and R. Deblock, *Phys. Rev. Lett.* **108**, 046802 (2012).
 - ²¹ B. S. Shastry, *Phys. Rev. B* **73**, 085117 (2006).
 - ²² B. S. Shastry, *Reports on Progress in Physics* **72**, 016501 (2009).
 - ²³ W. Xu, C. Weber, and G. Kotliar, *Phys. Rev. B* **84**, 035114 (2011).
 - ²⁴ Mahan, G. D., *Many-Particle Physics* (Kluwer Academic, New York, 2000).
 - ²⁵ J. M. Luttinger, *Phys. Rev.* **135**, A1505 (1964).
 - ²⁶ F. D. M. Haldane, *Phys. Rev. Lett.* **40**, 416 (1978).
 - ²⁷ A. C. Hewson, *The Kondo Problem to Heavy Fermions* (Cambridge University Press, Cambridge, 1993).
 - ²⁸ H. R. Krishna-murthy, J. W. Wilkins, and K. G. Wilson, *Phys. Rev. B* **21**, 1003 (1980).
 - ²⁹ H. R. Krishna-murthy, J. W. Wilkins, and K. G. Wilson, *Phys. Rev. B* **21**, 1044 (1980).
 - ³⁰ R. Bulla, T. A. Costi, and T. Pruschke, *Rev. Mod. Phys.* **80**, 395 (2008).
 - ³¹ We used the open-access Budapest Flexible DM-NRG code, <http://www.phy.bme.hu/~dmnrg/>; O. Legeza, C. P. Moca, A. I. Tóth, I. Weymann, G. Zaránd, arXiv:0809.3143 (2008) (unpublished).
 - ³² P. Nozières, *Journal of Low Temperature Physics* **17**, 31 (1974).
 - ³³ T. A. Costi and A. C. Hewson, *Journal of Physics: Condensed Matter* **5**, L361 (1993).
 - ³⁴ L. Glazman and M. Pustilnik, *New Directions in Mesoscopic Physics (Towards Nanoscience)*, NATO Science Series, **125**, 93 (2003).
 - ³⁵ V. Körting, Ph.D. thesis, Karlsruhe University, 2007.